Geoderma 376 (2020) 114560

Contents lists available at ScienceDirect

Geoderma

journal homepage: www.elsevier.com/locate/geoderma

Estimation of annual CO_2 efflux of moss biocrust through measuring and simulating its respiration rate in a semiarid climate

Xiaomeng Yao[a,b], Matthew A. Bowker[c], Bo Xiao[a,b,*]

[a] College of Land Science and Technology, China Agricultural University, Beijing 100193, China
[b] State Key Laboratory of Soil Erosion and Dryland Farming on the Loess Plateau, Institute of Soil and Water Conservation, Chinese Academy of Sciences and Ministry of Water Resources, Yangling, Shaanxi 712100, China
[c] School of Forestry, Northern Arizona University, Flagstaff 86011, USA

ARTICLE INFO

Handling editor: Jan Willem Van Groenigen

Keywords:
Biological soil crust
Soil carbon efflux
Soil carbon storage
Soil moisture
Soil temperature
Chinese Loess Plateau

ABSTRACT

Biocrust is a potentially extensive living cover in drylands, which comprises much of the land surface, but presently its contribution to the soil respiration rate (R_s) and CO_2 efflux is still not clearly understood. In this study, we continuously measured the R_s of moss-dominated biocrust (biocrust and biocrust covered soil) and bare soil, together with soil temperature and moisture, for ~100 days each in a semiarid climate on the Chinese Loess Plateau. We modeled R_s across a two-year period, based on its relationship with soil temperature and moisture. Using the model, the seasonal variation of the R_s was simulated for biocrust and bare soil, and their annual CO_2 efflux were further estimated. We also obtained samples of the biocrust layer and bare soil surface and analyzed their physicochemical properties and enzyme activities to explain the biocrust effects on R_s. Our results showed that the measured R_s of the biocrust and bare soil ranged from 0.05 to 7.62 and 0.02–2.73 μmol m^{-2} s^{-1}, respectively, and was closely exponentially related to the dynamics of soil temperature and moisture (in threshold relationships). The variations of R_s in both the biocrust and bare soil were strongly predicted in a regression model by $R^2 \geq 0.50$ and $P < 0.001$. Through this model, we simulated the seasonal variations of R_s, which averaged 1.03 ± 0.01 and 0.54 ± 0.01 μmol m^{-2} s^{-1} ($F = 225.51$, $P < 0.001$) across all seasons for the biocrust and bare soil, respectively. We further estimated that the annual CO_2-C efflux through respiration of the biocrust was 390 g m^{-2} yr^{-1} and that of the bare soil was 203 g m^{-2} yr^{-1}, indicating that the presence of the biocrust layer annually contributed 91.8% (187 g m^{-2} yr^{-1}) more soil respiration in comparison to the bare soil. Moreover, the main correlates with R_s shifted from largely abiotic, e.g. soil texture and total phosphorus content, in bare soils to biotic, e.g. indicators of carbon and nitrogen content, in biocrust soils. This finding implies that the contribution of the biocrust to R_s is linked to the carbon fixed and organic nutrients stored in the biocrust layer. In conclusion, moss-dominated biocrust highly accelerates soil respiration and increases gross soil CO_2 efflux, possibly through regulating soil temperature and moisture, improving soil physicochemical properties, increasing soil enzyme activities, and accelerating decomposition of biocrust-fixed and -stored carbon.

1. Introduction

Drylands occupy up to ~41% of the Earth's land surface; thus, they may regulate both the long-term trajectory and interannual variability of the global terrestrial carbon (C) sink (Lal, 2004; Poulter et al., 2014). As a main component of CO_2 efflux from ecosystems to the atmosphere (Leon et al., 2014), soil respiration is mostly generated from three sources (Bond-Lamberty et al., 2011): a) autotrophic respiration by, e.g., roots, b) heterotrophic respiration by microorganisms and soil fauna that acts as decomposers or root symbionts, and c) chemical oxidation of C-containing material. Soil respiration rate (R_s) is the rate of amount of C efflux from soils, and it is of particular concern in the estimation of aboveground and underground debris production and root respiration rates. In terrestrial ecosystems, the soil C efflux from respiration is estimated at ~94 Pg C yr^{-1} (Xu and Shang, 2016), which accounts for over a quarter of global C emission, and 10 times more than fossil fuel burning (Raich et al., 2002). Therefore, even minor changes in R_s may have a global impact on atmospheric CO_2

* Corresponding author at: College of Land Science and Technology, China Agricultural University, No. 2, Yuanmingyuan West Road, Haidian District, Beijing 100193, China.
E-mail address: xiaobo@cau.edu.cn (B. Xiao).

https://doi.org/10.1016/j.geoderma.2020.114560
Received 7 January 2020; Received in revised form 23 June 2020; Accepted 26 June 2020
Available online 11 July 2020

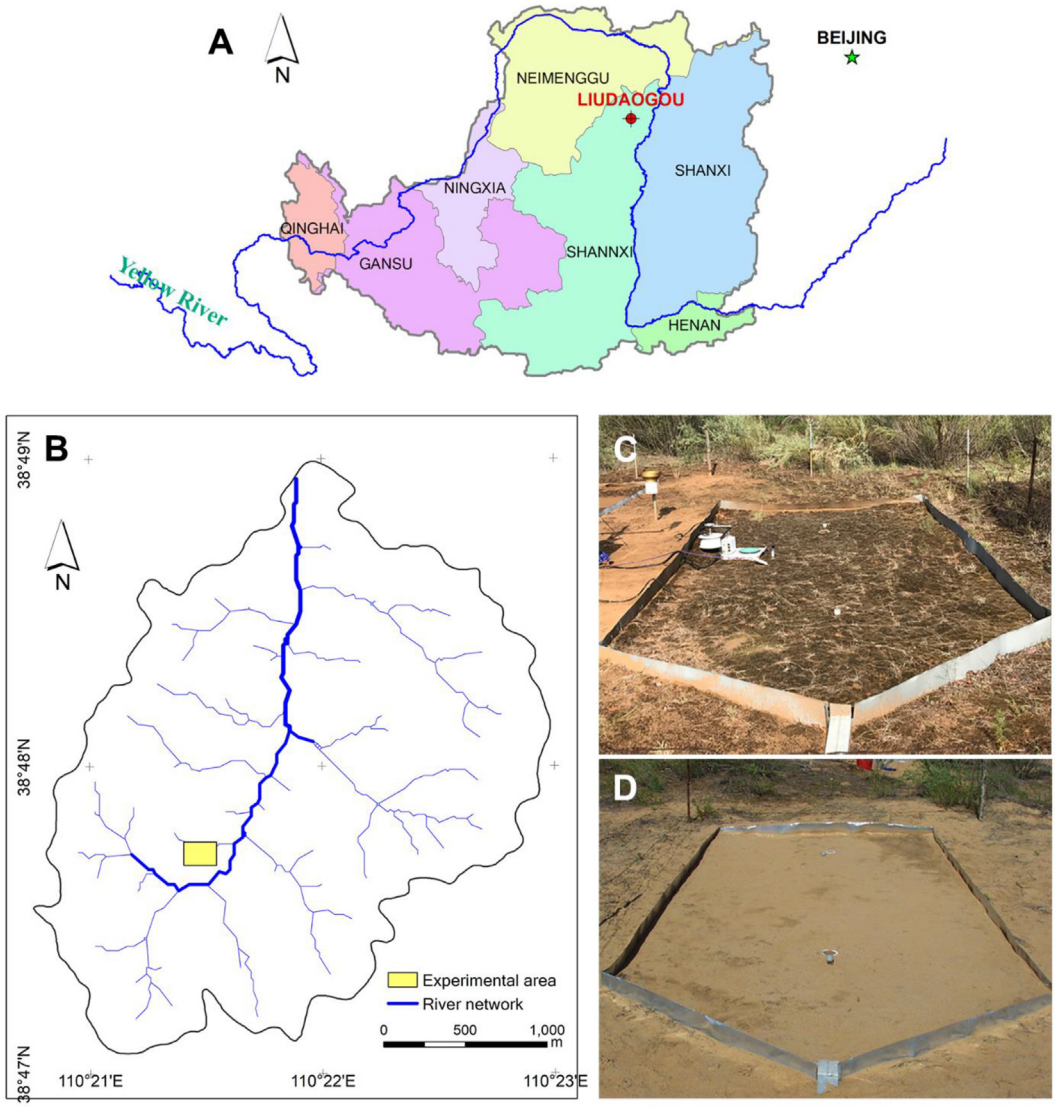

Fig. 1. Location of (A) the Liudaogou watershed, (B) the experimental area, and the plots of biocrust (C) and bare soil (D).

concentration and climate variation (Schindlbacher et al., 2012). Although R_s is fundamentally determined by the amount of different forms of C stored in soil as well as the abundance and activity of soil microbes, many environmental factors, particularly soil temperature and moisture, have indirect but significant influences on R_s (Hursh et al., 2017).

Biocrust (also called biological soil crust) is a major photosynthetic component of dryland ecosystems worldwide residing in the upper few millimeters to centimeters of the soil surface, commonly composed of cyanobacteria, lichens, mosses, other bacteria, micro-fungi, and the soil particles they aggregate (García-Palacios et al., 2018). Biocrust is a critical factor in changing hydrology and soil moisture (Chamizo et al., 2012a; Xiao et al., 2019b), altering surface albedo and temperature (Rutherford et al., 2017; Xiao et al., 2019a), maintaining soil stability (Belnap and Büdel, 2016), decreasing soil erosion (Chamizo et al., 2017; Gao et al., 2020), and affecting global cycles of C and nitrogen (N) (Elbert et al., 2009; Elbert et al., 2012). Particularly, biocrust directly and indirectly influences the dynamics of soil CO_2 flux through their own photosynthesis and respiration, and by providing habitat and resources for heterotrophic microbes (Castillo-Monroy et al., 2011; Kidron et al., 2015). Moreover, biocrust can create a stable environment for soil microorganisms by altering soil environmental factors, especially moisture and temperature (Xiao et al., 2016), further influencing R_s by modifying the activity of microbes. Due to the multiple pathways by which biocrust can influence soil respiration and the importance of soil respiration in C cycling in drylands, it is important to elucidate the role played by biocrust in regulating R_s; to date, this subject has been understudied.

It is commonly believed that biocrust has a powerful influence on soil CO_2 efflux dynamics in arid and semiarid ecosystems (Morillas et al., 2017; Yao et al., 2019), mostly owing to the following two reasons. First, the photoautotrophics components (e.g., cyanobacteria, lichens, and mosses) of biocrust enhance the R_s of biocrust covered soil by boosting autotrophic respiration over what would be expected on bare soil (Castillo-Monroy et al., 2011; Yu et al., 2014). More importantly, although biocrust may have lower R_s compared with vascular plants per unit area, their total contribution to soil respiration in arid and semiarid climate regions could be greatly amplified by their relatively high cover, which makes up to 12% of Earth's terrestrial surface (Rodríguez-Caballero et al., 2018). Therefore, the contribution of biocrust to soil respiration must be sufficiently evaluated in assessing C balance of drylands, but presently we only have a very limited knowledge about the variation in this contribution and relevant controlling factors. Furthermore, although the influences of biocrust on soil physicochemical properties and enzyme activities have been investigated in different regions (Chamizo et al., 2012b; Liu et al., 2014),

their connections with soil respiration are still not fully elucidated, likely a critical knowledge gap for understanding the mechanisms of biocrust effects on soil respiration in drylands.

In this study, we hypothesized that the presence of biocrust would significantly increase R_s in comparison to bare soil in drylands, and that the increase in R_s can be well explained by the changes in soil physicochemical properties and enzyme activities, especially the regimes of soil temperature and moisture. Based on these hypotheses, we continuously measured the R_s of moss-dominated biocrust and bare soil as well as their temperature and moisture for ~100 days on the Chinese Loess Plateau. We also established a regression model of R_s for biocrust and bare soil and estimated their annual CO_2 efflux through simulating the variation of R_s over two years. We further analyzed biocrust effects on soil physicochemical properties and enzyme activities as well as their correlations with R_s. Our specific objectives were: 1) to evaluate the contribution of biocrust to soil respiration through comparing the R_s of biocrust with that of bare soil under different environmental conditions, 2) to estimate the annual CO_2 efflux of biocrust based upon the measured and simulated R_s over two years, and 3) to understand the regulating mechanisms of biocrust on soil respiration through analyzing the relationships between R_s and soil physicochemical properties, as well as soil enzyme activities. Our study provides new insights into the factors that regulate R_s in biocrust and also the estimation of annual CO_2 efflux of moss-dominated biocrust in drylands with semiarid climate.

2. Materials and methods

2.1. Study area

The measurements were performed in the Liudaogou watershed on the Northern Chinese Loess Plateau (Fig. 1A–B), located at 38°46′–38°51′ N, 110°21′–110°23′ E, at an altitude of 1,081–1,274 m. The region is characterized by a semiarid climate, where the mean annual precipitation is 409 mm and the mean annual water evaporation is 1,337 mm. The mean annual temperature is 8.4 °C, and the mean monthly temperature ranges from –9.7 °C in winter (December–February) to 23.7 °C in summer (June–August) (Xiao et al., 2016). The main land use was as a soil conservation reserve with shrubs including *Salix psammophila*, *Artemisia desertorum*, and *Medicago sativa*, with a coverage of about 30%. The soil texture is mostly sandy, and the soil is classified as a Psamment (specifically an aeolian sandy soil) according to the USDA soil taxonomy (Soil Survey Staff, 1999).

2.2. Sampling and measurements

Two treatments (biocrust and bare soil) were considered in this study, and each treatment had five replicates. The biocrust (~30 years old and containing > 95% moss cover; the dominant moss species were *Bryum argenteum* Hedw. and *Didymodon vinealis* (Brid.) Zander) was naturally developed on fixed aeolian sand after vegetation restoration in the Grain for Green program, while the bare soil surface was located further away from vegetation and thus had suffered wind and water erosion. Except for the presence or absence of the biocrust layer, the two treatments had quite similar conditions and topography (in a south-oriented slope with gradient < 9%).

We chose five sites in the study area for establishing biocrust (Fig. 1C) and bare soil (Fig. 1D) plots (3 m × 5 m in area; at least 3 m away from each other, and at least 5 m distant from the nearest shrub to minimize root respiration). The biocrust plots were located at very similar landscape positions as compared with the bare soil plots; all the plots of the two treatments were distributed in a sparse shrubland with an area of about 1 ha. In each plot, a soil collar (20 cm diameter, 10 cm height) was inserted at least one day ahead of the initiation of the measurements. The R_s and soil temperature and moisture were continuously measured every 30 min for ~100 days in total by the LI-8100A automated soil respiration system (LI-COR, Inc., USA). Specifically, the measurements of R_s for the biocrust were performed in 104 days from June 16 to September 28, 2017, while that for the bare soil were performed in 90 days from May 8 to August 5, 2018. The soil temperature and moisture were measured at depths of 2 and 5 cm by 5TE sensors (METER Group, Inc., USA) controlled by a CR3000 micrologger (Campbell Scientific, Inc., USA), and they spanned the whole period from June 18, 2017 to August 15, 2018. Thus, the R_s was measured simultaneously in the five biocrust plots in the first year and in the five plots of bare soil in the second year, and the soil temperature and moisture of the biocrust and bare soil plots were continuously measured within the two years.

Samples (depth of ~2 cm) of the biocrust and bare soil of each plot were taken using Petri dishes in the same year as the respiration measurements, and their physicochemical properties as well as enzyme activities were analyzed in the laboratory through the following methods. First, the soil particle-size distribution of the samples was determined through a Mastersizer 2000 laser particle-size analyzer (Malvern Instruments Ltd., UK); the bulk density of the biocrust layer and bare soil were measured using the immersion method in water (Makhuvha et al., 2014) and cutting ring (100 cm^3), respectively. Secondly, the organic C (OC) was determined with the oil bath-$K_2Cr_2O_7$ titration method (oxidization with dichromate in presence of H_2SO_4, heated at 180 °C for 5 min (Li et al., 2010); the labile organic C (LOC) was measured by the $KMnO_4$-$CaCl_2$ (0.1 M) oxidized method (Weil et al., 2003); the microbial biomass C (MBC) and microbial biomass N (MBN) were measured using the $CHCl_3$ fumigation extraction method, which were calculated from the difference between the amount of total C and N extracted by 0.5 M K_2SO_4 from fresh soil fumigated with $CHCl_3$ and the amount extracted from the unfumigated control soil (Sparling and West, 1988). Moreover, the total N (TN) was measured by the method of micro-Kjeldahl digestion followed by steam distillation (Carter and Gregorich, 2006); the available N (AN; NO_3-N) was extracted by 2.0 M KCl and measured using the continuous flow auto analyzer (Carter and Gregorich, 2006). Additionally, the total phosphorus (TP) was digested with H_2SO_4 and $HClO_4$ and measured by spectrophotometer (Parkinson and Allen, 1975); the available P (AP) was extracted by 0.5 M $NaHCO_3$ and measured using the molybdate method (Liu et al., 2010).

Lastly, the soil enzyme activities of the samples were measured by the procedures described as follows.

1) Urease activity: 5 g of air-dried sample was mixed with 1.5 mL of C_7H_8, 10 mL of citrate buffer solution (0.1 mol L^{-1}; pH = 6.7), and 5 mL of substrate solution (10% (w/v) urea) in a reaction flask and incubated at 37 °C for 24 h. After incubation, the culture solutions were added to 100 mL of distilled water (38 °C) and filtered after complete mixing. Then 1 mL of the filtrate was added into the reaction solutions (4 mL of 0.1 mol L^{-1} phenolate and 3 mL of 0.9% hypochlorite). The mixtures were filtered again, and the final filtrates were spectrophotometrically determined at 578 nm (Yao et al., 2006).
2) Sucrase activity: 2 g of air-dried sample was mixed with 15 mL of sucrase solution (8%), 5 mL of phosphate buffer (pH = 5.5), and 5 drops of C_7H_8. The flask was shaken and then incubated at 37 °C for 24 h. After incubation, the sample was filtered; 0.5 mL of the filtrate and 1.5 mL of salicylic acid were taken into a 25-mL test tube and heated for 5 min at 100 °C in a water bath. After that, the test tube was cooled for 3 min with running tap water and subsequently was filled by deionized water to a total volume of 25 mL. The sucrase activity was measured spectrophotometrically at 508 nm (Ge et al., 2010).
3) Protease activity: 5 g of air-dried sample and 10 mL of 1% gelatin solution (0.2 mol L^{-1} phosphate buffer; pH = 7.4) was mixed and incubated at 30 °C for 24 h. Then, 0.5 mL of H_2SO_4 (0.05 mol L^{-1}) and 3 mL of Na_2SO_4 (20%) were added into the filtrate to precipitate

the residual protein. The mixed solution was filtered again, and 5 mL of the final filtrate was used to analyze the protease activity at 560 nm by a spectrophotometer (Wu et al., 2004).

4) Polyphenol oxidase and peroxidase activity: 1 g of sample was added into 125 mL of acetate buffer (50 mmol L^{-1}; pH = 5.0) and homogenized for 1 min. Then, 50 μL of L-3, 4-dihydroxyphenylalanine (DOPA; 25 mmol L^{-1}) was added into each polyphenol oxidase sample, while 50 μL of DOPA and 10 μL of H_2O_2 (0.3%) were added into each peroxidase sample. After that, the samples were incubated in dark at 20 °C for 18 h, and their enzyme activities were quantified by measuring absorbance at 450 nm (Saiya-Cork et al., 2002).
5) Alkaline phosphatase activity: 0.5 g of sample was added into 2 mL of sodium acetate buffer (0.5 mol l^{-1}; pH = 11.0) and 0.5 mL of p-nitrophenyl phosphate disodium (PNPP; 0.15 mol L^{-1}) and incubated at 37 °C for 1 h. Then, 0.5 mL of $CaCl_2$ (0.5 mol L^{-1}) and 2 mL of NaOH (0.5 mol L^{-1}) were added into the solutions and centrifuged. The resultant p-nitrophenol was determined by spectrophotometry at 398 nm (Liu et al., 2010).
6) Catalase activity: 5 g of sample was mixed with 40 mL of distilled water and 5 mL of H_2O_2 (0.3%). The mixture was incubated at 37 °C for 20 min. After that, 5 mL of H_2SO_4 (3 mol L^{-1}) was injected into the flask for stopping the reaction inside and the reaction solution was then filtered. Then, 2.5 mL of filtrate was titrated with $KMnO_4$ (0.1 mol L^{-1}) solution, judging the color change from colorless to slight red color. The consumed amount of $KMnO_4$ per gram of dried sample was used to express the activity of catalase (Min et al., 2001).

2.3. Data analysis

After normality and equality of variance tests, repeated measures ANOVA was performed to test the differences between the biocrust and bare soil ($\alpha = 0.05$) in R_s, soil temperature and moisture, because these data were re-measured many times on the same sample units. We statistically tested the differences in the physicochemical properties and enzyme activities between the two treatments ($\alpha = 0.05$) using the independent-samples *t*-test because these measurements were only implemented one time. The two-way repeated measures ANOVA (crust and month, as well as their interaction effect) was also performed to test the differences in the simulated R_s between the two treatments as different seasons were included through simulating R_s within two years (simulation details are provided in the following paragraph). Afterwards, the differences in R_s and soil CO_2-C efflux between the biocrust and bare soil were analyzed to evaluate the contribution of biocrust to soil respiration and annual CO_2-C efflux. We obtained Spearman correlations between the averaged daily R_s and soil physicochemical properties, or enzyme activities, to explore the regulating mechanisms underlying biocrust effects on soil respiration. Spearman correlation was suited to our purposes because it can detect monotonic correlations whether they are linear or not.

To select a model of R_s with soil temperature and moisture for the simulations mentioned above, we conducted a thorough review of soil respiration models proposed by other scientists and fitted these univariate and bivariate models (Jiang et al., 2013). The performances of these models were evaluated by their coefficient of determination (R^2) and bias in the distribution of the residuals. Our results indicated that the univariate and bivariate models listed in Eqs. (1) and (3–4) were the best regression models for biocrust and bare soil respiration in our study, a finding also demonstrated in our previous work (Yao et al., 2019). The nonlinear curve fitting was performed using OriginPro 2020 based on Eqs. (1) and (3–4) to obtain the relationships between the R_s and soil environmental factors (temperature and moisture).

The relationship between the R_s (μmol m^{-2} s^{-1}) and soil temperature (*T*, °C) was fitted with an exponential function (Lloyd and Taylor, 1994):

$$R_s = R_0 \times e^{aT} \quad (1)$$

where R_0 is the basal R_s at 0 °C (μmol m^{-2} s^{-1}); a is a constant for a given soil surface, which comes from the fitting results and is used to calculate Q_{10} through Eq. (2). The Q_{10} describes the sensitivity of R_s to soil temperature, which is defined as the increment in R_s when temperature increases by 10 °C (Qi et al., 2002).

$$Q_{10} = e^{10a} \quad (2)$$

Similarly, the relationship between the R_s and soil moisture (θ, cm^3 cm^{-3}) was fitted with the following piecewise function (Doran et al., 1990; Tang et al., 2006):

$$R_s = \begin{cases} a + b\theta + c\theta^2, & \theta < \theta_0 \\ a + b\theta, & \theta \geqslant \theta_0 \end{cases} \quad (3)$$

where θ_0 is the inflexion point of soil moisture (cm^3 cm^{-3}), below which R_s has almost no response to moisture changes; a, b, c are fitting parameters without specific meaning.

Furthermore, the relationships among the R_s and soil temperature and moisture were fitted with the following regression model (Yao et al., 2019):

$$R_s = a \times e^{-0.5[((T-T_0)/b)^2+((\theta-\theta_0)/c)^2]} \quad (4)$$

where T_0 is the inflexion point of soil temperature (°C), below which R_s has no response to temperature changes. In Eq. (4), the values of T_0, θ_0, a, b, and c were obtained through the nonlinear curve fitting in OriginPro 2020.

Finally, the variations of R_s in every 30 min during the period from June 18, 2017 to August 15, 2018 were simulated through Eq. (4) with the measured soil temperature and moisture, as well as the fitting parameters obtained in the regression model. From the simulated R_s in every 30 min, the daily soil CO_2-C efflux (*F*, g m^{-2} d^{-1}) was calculated through Eq. (5) in different seasons, and then the annual amount of CO_2-C efflux (*AF*, g m^{-2} yr^{-1}) was further estimated through summation in Eq. (6).

$$F = \sum_{1}^{48} R_s/48 \times 3600 \times 24 \times 12 \times 10^{-6} \quad (5)$$

$$AF = \sum_{1}^{365} F \quad (6)$$

3. Results

3.1. Measured R_s of biocrust and bare soil

As presented in Fig. S1, the R_s in the biocrust and bare soil strongly fluctuated with time due to the changes of air temperature and rainfall events. Specifically, the R_s of the biocrust ranged from 0.05 to 7.62 μmol m^{-2} s^{-1} (Fig. S1A), while that of the bare soil only ranged from 0.02 to 2.73 μmol m^{-2} s^{-1} (Fig. S1B). During the measurement periods, the mean value of the R_s of biocrust and bare soil were 2.12 and 0.77 μmol m^{-2} s^{-1}, respectively, showing that the biocrust averaged 2.75 times higher R_s than that of the bare soil (Fig. 2A). The results of a repeated measures ANOVA showed that the differences in the measured R_s between the biocrust and bare soil were significant. However, we should be aware that the climatic conditions between the two measurement periods for the biocrust (in 2017) and bare soil (in 2018) were not identical. As shown in Fig. 2, the measurement period for biocrust in 2017 was slightly colder (0.9 °C of air temperature on average; Fig. 2B) but much wetter (202.8 mm of rainfall in total; Fig. 2C) in comparison to the measurement period for bare soil in 2018. These differences in climate led to key differences in the soil environment in the two measurement periods. The biocrust soil, for example, had a 2.5 °C lower soil temperature on average (Fig. 2D) and 0.03 cm^3

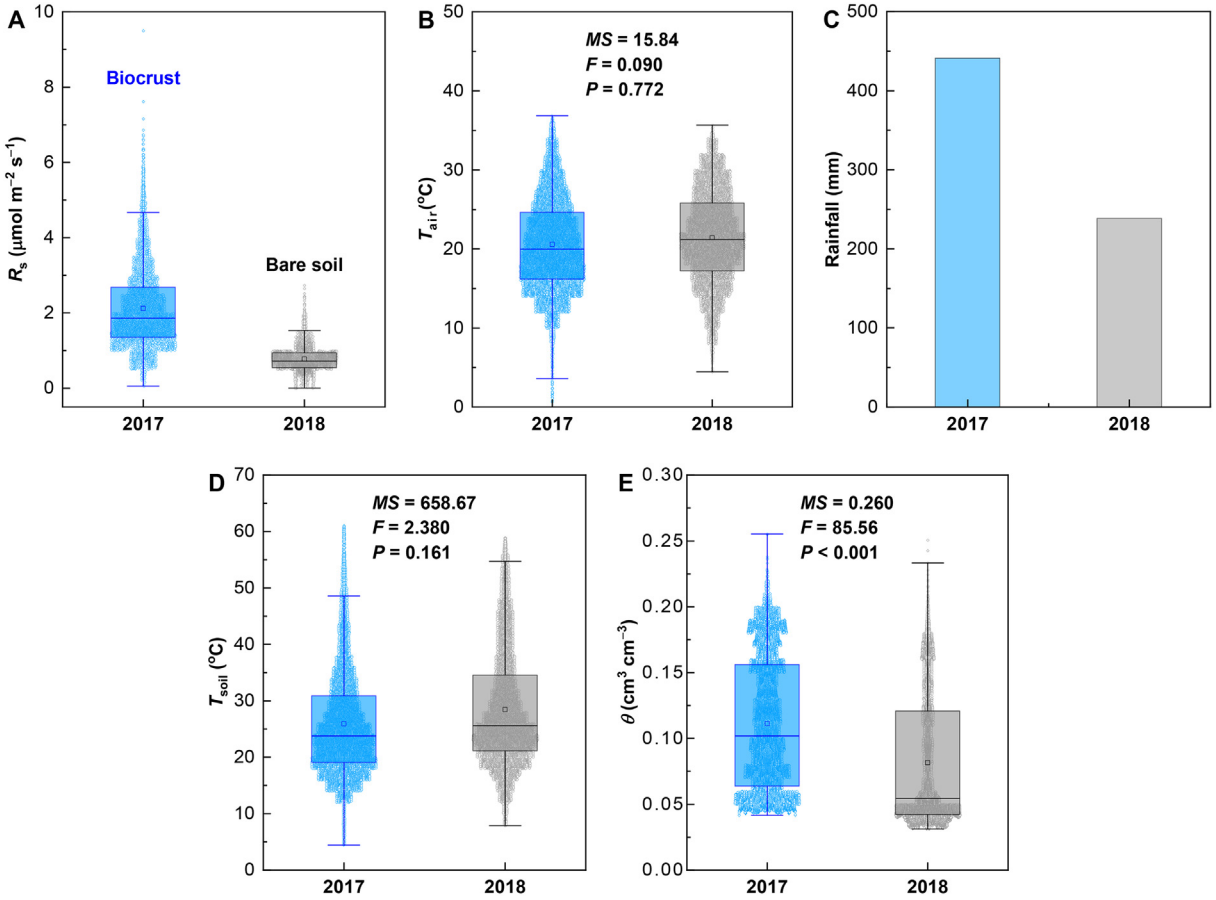

Fig. 2. Measured soil respiration rate (R_s) of the biocrust in 2017 and that of the bare soil in 2018, as well as the comparison of climatic conditions between the two measurement periods in 2017 and 2018. (A) R_s; (B) Air temperature (T_{air}); (C) Rainfall; (D) Soil temperature (T_{soil}) of the biocrust at depth of 2 cm; (E) Soil moisture (θ) of the biocrust at depth of 2 cm. *MS* = Mean Square.

cm^{-3} higher soil moisture (Fig. 2E) at a depth of 2 cm in 2017 compared to 2018. Moreover, the R_s of biocrust strongly fluctuated within and among days owing to wide changes of air temperature and rainfall events (Fig. S1A), while that of the bare soil fluctuated much more gently (Fig. S1B). Accordingly, the coefficient of variation of the biocrust and bare soil were 0.52 and 0.43, respectively. Nevertheless, we obtained sufficient variation in environmental conditions for both biocrust and bare soil on which to base a model of R_s and allow a comparison of values during the same time periods.

3.2. Simulation of R_s for biocrust and bare soil

The R_s of the biocrust and bare soil both had weak responses (slope = 0.005–0.007) to the changes in soil temperature under dry conditions (see Fig. S2), but they immediately had very strong exponential relationships (sharp increases) with soil temperature in sufficient water conditions (Fig. 3), especially for the biocrust ($R^2 \geq 0.63$; Fig. 3A–B). As indicated by the experimental data in Fig. 3, the inflexion points of the soil moisture at which the relationship of R_s with soil moisture changes from positive to negative were approximately 0.15 and 0.11 cm^3 cm^{-3} for the biocrust and bare soil, respectively. According to the R^2 presented in Fig. 3, the R_s of biocrust was better explained by the soil temperature at depth of 2 cm than that at depth of 5 cm, while the R_s of bare soil was well explained by the soil temperature at depth of 5 cm rather than that at depth of 2 cm. Thus, these specific soil depths were selected for the biocrust and bare soil in further analysis and modeling. In wet conditions, our regression results implied that the soil temperature explained 70.5% of the variance in the R_s of the biocrust, while the soil temperature explained only 19.2% of the variance in the R_s of the bare soil (Fig. 3). In our study, the sensitivity of R_s to soil temperature, Q_{10}, was 1.88 and 1.97 for the biocrust (Fig. 3A) and bare soil (Fig. 3D), respectively. Additionally, during the periods of measurements, the biocrust had 0.78 °C higher soil temperature on average in comparison to the bare soil.

As shown in Fig. 4, the relationships between the R_s and soil moisture were divided into two stages by the inflexion point of soil moisture both in the biocrust and bare soil: in the first stage the R_s was positively correlated with the soil moisture, but in the second stage the R_s was negatively correlated with the soil moisture. The relationships between the R_s and soil moisture were well fitted with quadratic functions in the first stage ($R^2 \geq 0.20$), and they were well fitted with linear functions in the second stage ($R^2 \geq 0.83$). Similarly to the results of soil temperature in Fig. 3, we used only the soil moisture at depth of 2 cm for the biocrust (Fig. 4A) and that at depth of 5 cm for the bare soil (Fig. 4D) in further analyses mostly due to their higher R^2 compared to that at the other soil depths (Fig. 4B–C). From Fig. 4, we estimated that the inflexion points of soil moisture were ~0.15 cm^3 cm^{-3} for the biocrust and were ~0.11 cm^3 cm^{-3} for the bare soil. As indicated by the R^2 in Fig. 4, the soil moisture (at depth of 2 cm for the biocrust and of 5 cm for the bare soil) explained 29.1% and 28.3% of the variance in the R_s of the biocrust and bare soil, respectively, in the first stage; while in the second stage the soil moisture (at depth of 2 cm for the biocrust and of 5 cm for the bare soil) explained 83.4% and 86.8% of the variance in the R_s of the biocrust and bare soil, respectively. In addition, the biocrust averaged 0.04 cm^3 cm^{-3} higher soil moisture in comparison to the bare soil.

In order to simultaneously evaluate the responses of the R_s to the changes of soil temperature and moisture, we modeled the R_s based on

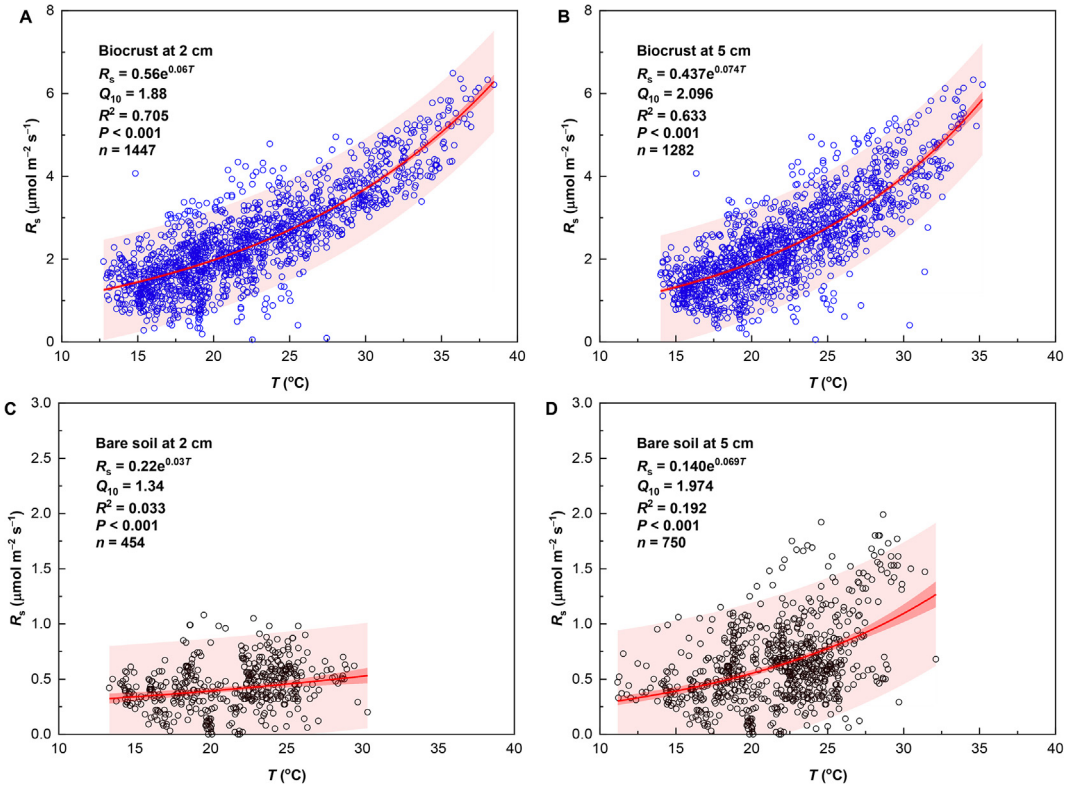

Fig. 3. Relationships between the measured soil respiration rate (R_s) and soil temperature (T) for the biocrust and bare soil in optimal water conditions (biocrust ≥ 0.15 cm^3 cm^{-3}; bare soil ≥ 0.11 cm^3 cm^{-3}). (A) R_s vs. T at depth of 2 cm for biocrust; (B) R_s vs. T at depth of 5 cm for biocrust; (C) R_s vs. T at depth of 2 cm for bare soil; (D) R_s vs. T at depth of 5 cm for bare soil. The shaded area represents the confidence and prediction bands at the 95% confidence-level.

the corresponding soil temperature and moisture through a nonlinear curve fitting listed in Eq. (4) (see Fig. 5). Due to the results shown in Figs. 3–4, the soil temperature and moisture at depth of 2 cm were selected for the curve fitting of biocrust, while that at depth of 5 cm were selected for the curve fitting of bare soil. As indicated by the R^2, the combination of soil temperature and moisture explained 52.7% and 50.4% of the variance in the R_s of the biocrust (Fig. 5A) and bare soil (Fig. 5B). The value of R^2 in Fig. 5 and the regression results in Table 1 indicated that the R_s of the biocrust and bare soil were both well predicted by our model. The results listed in Table 1 also showed that the biocrust had a lower (1.3 °C) inflexion point of soil temperature but a higher (0.04 cm^3 cm^{-3}) inflexion point of soil moisture as compared with the bare soil.

3.3. Simulated R_s and estimated annual CO_2 efflux of biocrust and bare soil

According to the regression functions listed in Table 1 and Fig. 5, we simulated the seasonal variations of the R_s in every 30 min during the period from June 18, 2017 to August 15, 2018 with the measured soil temperature and moisture (Table 2 and Fig. 6). From Fig. 6, we found that both the biocrust and bare soil had much higher R_s in hot and wet conditions in summer, while they had very low R_s in dry and cold conditions in winter (the period marked as yellow in Fig. 6). During the period of a whole year (from June 18, 2017 to June 17, 2018), the simulated R_s averaged 1.03 ± 0.01 and 0.54 ± 0.01 μmol m^{-2} s^{-1} (F = 225.51, P < 0.001) for the biocrust and bare soil across all seasons, respectively (Fig. 7A). The simulated R_s of both the biocrust and bare soil had similar seasonal variation pattern, which gradually increased from January to August and then decreased from August to December (Fig. 7B). However, the biocrust consistently and significantly had higher R_s than the bare soil in identical climatic conditions across the whole year (Fig. 7B). From the simulated R_s estimated every 30 min (Fig. 6), we calculated the daily soil CO_2-C efflux and then estimated the annual amount of CO_2-C efflux, which was 390 and 203 g m^{-2} yr^{-1} for the biocrust and bare soil, respectively (Table 2 and Fig. 7C). In other words, the biocrust annually contribute 91.8% (187 g m^{-2} yr^{-1}) more soil C efflux in comparison to the bare soil.

3.4. Correlations between R_s and soil physicochemical properties or enzyme activities

As listed in Table 3, the biocrust layers had significant lower content of sand particles (13.7%) but higher content of silt (121%) and clay (136%) as compared with the bare soil. Subsequently, they had much lower (26.1%) bulk density than the bare soil. Moreover, the contents of different forms of C (OC, LOC, and MBC), N (TN, AN, and MBN), and P (TP and AP) of the biocrust were consistently higher (1.51–6.40, 1.13–4.18, and 1.05–5.65 times higher for C, N, and P, respectively) than that in the bare soil. Similarly, the biocrust had much higher (1.48–31.89 times higher) activities in all types of soil enzymes in comparison to the bare soil (Table 3). In addition, the strength and sign of correlations between R_s and various soil properties differed in biocrust and bare soil (Table 4). In biocrust, TN was the strongest positive correlate among the soil properties, and other indicators of organic matter and fertility were influential (Table 4). Among the enzyme activities, alkaline phosphatase was notable as a negative correlate with R_s in biocrust (Table 5). In bare soils, R_s was most strongly and positively correlated with the percentage of sand, and negatively correlated with TP (Table 4); among the soil enzymes, urease activity was the strongest negative correlate (Table 5).

4. Discussion

4.1. Biocrust strongly enhances the magnitude of soil respiration

As we expected in this study, we found that the moss-dominated

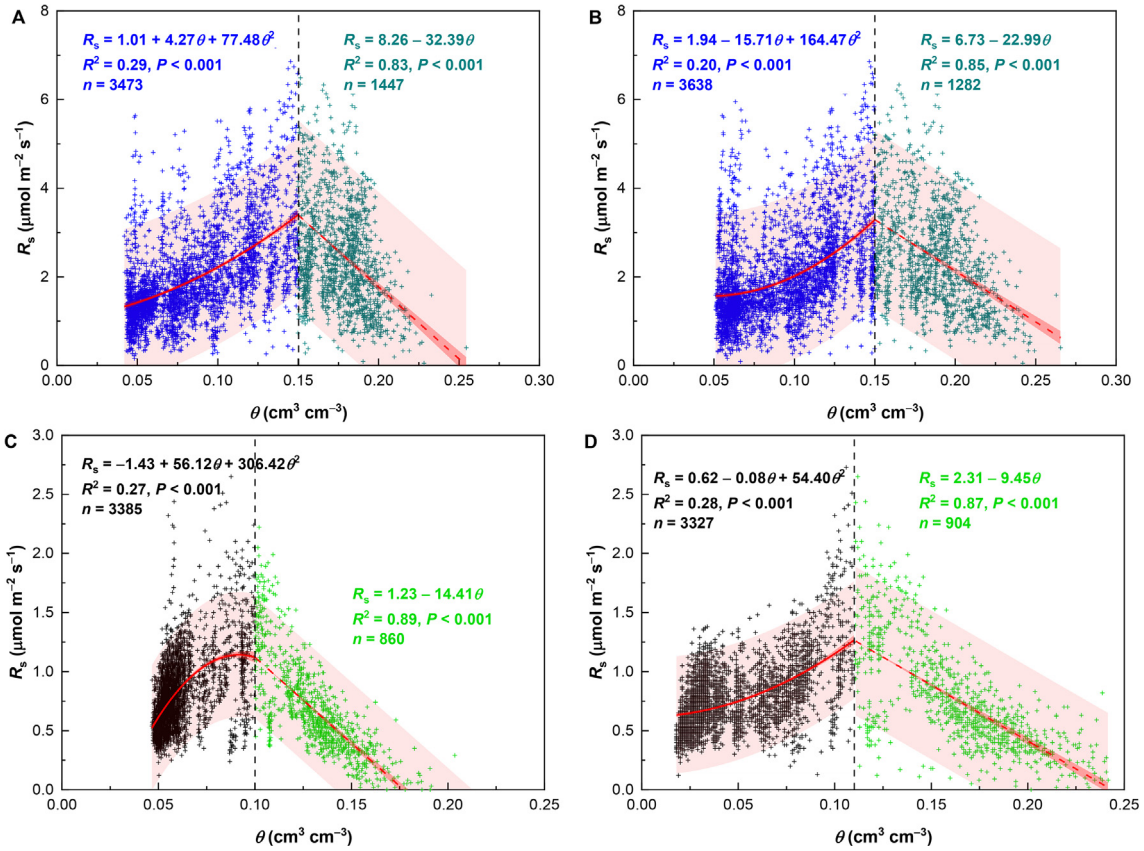

Fig. 4. Relationships between the measured soil respiration rate (R_s) and soil moisture (θ) for the biocrust and bare soil. (A) R_s vs. θ at depth of 2 cm for biocrust; (B) R_s vs. θ at depth of 5 cm for biocrust; (C) R_s vs. θ at depth of 2 cm for bare soil; (D) R_s vs. θ at depth of 5 cm for bare soil. The shaded area represents the confidence and prediction bands at the 95% confidence-level.

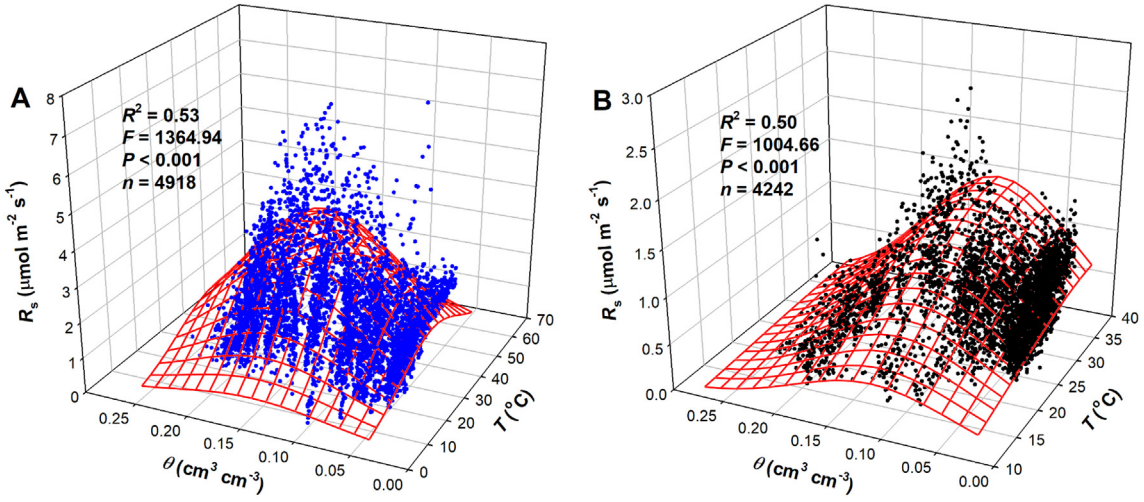

Fig. 5. Nonlinear curve fitting of the variations of measured soil respiration rate (R_s) to the changes of soil temperature (T) and moisture (θ) for the biocrust (A) and bare soil (B), respectively. The soil temperature and moisture at depth of 2 cm was selected for the curve fitting of biocrust, while that at depth of 5 cm were selected for the curve fitting of bare soil.

biocrust had a much higher R_s compared with the bare soil in the semiarid climate of the Chinese Loess Plateau. A higher R_s of biocrust has been previously reported in several climate regions around the world, but its degree of increase (1.01–1.20 times) in comparison to bare soil is highly dependent on the biocrust type (i.e., cyanobacterial-, lichen-, or moss-dominated biocrust; Gu et al., 2017), climate (e.g., hyper arid, arid, or semiarid; Chae et al., 2016; Morillas et al. 2017), and measurement timing and duration (e.g., different seasons; one time or continuous measurements across months; Chae et al., 2016; Xu and Qi, 2001). In comparison to the results of previous studies, we are reporting the highest increase in biocrust R_s compared to bare soil (1.91 times). This difference may be attributable to the dominance of mosses (rather than cyanobacteria, algae, or lichens) and the moderate environmental conditions of a semiarid climate (rather than arid or even hyper arid climates).

Although our R_s measurements were mostly performed in summer,

Table 1
Results of regression analysis using Eq. (4) based on the data of soil respiration rate (R_s) and corresponding soil temperature (T) and moisture (θ) of the biocrust and bare soil.

Regression parameter†	Biocrust						Bare soil					
	Value	Standard error	Lower limit‡	Upper limit‡	*F*	*P*	Value	Standard error	Lower limit	Upper limit	*F*	*P*
a	4.11	0.04	4.04	4.18	113.97	< 0.001	1.46	0.04	1.39	1.52	42.10	< 0.001
b	16.30	0.27	15.77	16.82	60.89	< 0.001	18.30	1.00	16.35	20.26	18.37	< 0.001
c	0.07	0.001	0.07	0.07	72.92	< 0.001	0.07	0.001	0.07	0.08	95.26	< 0.001
T_0	36.47	0.28	35.91	37.02	128.53	< 0.001	37.76	1.31	35.19	40.32	28.84	< 0.001
θ_0	0.15	0.001	0.15	0.15	167.39	< 0.001	0.11	0.001	0.11	0.11	162.90	< 0.001

† T_0 = the inflexion point of soil temperature (°C), below which R_s has almost no response to temperature changes; θ_0 = the inflexion point of soil moisture (cm^3 cm^{-3}), below which R_s has almost no response to moisture changes; and a, b, c are fitting parameters.
‡ The lower and upper limits are based on 95% confidence level.

we believe that we obtained sufficient variation in soil temperature and moisture due to the climate characteristics of our study area, where the air temperature is high at noon but can be very low (as low as ~0 °C in very early or late summer) in early morning and night in summer. The soil temperature of the biocrust and bare soil at depth of 2 cm ranged from 4.5 to 61.1 °C (Fig. S2A) and 8.7 to 50.5 °C (Fig. S2C), respectively, indicating that a sufficient wide range of temperature conditions had been included in our R_s measurements. Similarly, the soil moisture of the biocrust and bare soil at depth of 2 cm ranged from 0.03 to 0.26 cm^3 cm^{-3} (Fig. 4A) and 0.04 to 0.20 cm^3 cm^{-3} (Fig. 4C), respectively, implying that several complete soil dry-wet processes occurred during our measurements and providing sufficient variations of soil moisture. Moreover, as indicated by our best model of R_s in Eq. (4), the soil temperature and moisture had threshold values of 36.5 °C and 0.15 cm^3 cm^{-3} for biocrust and 37.8 °C and 0.11 cm^3 cm^{-3} for bare soil, respectively. These are the threshold values below which R_s has weak response to temperature and moisture changes but also the threshold values above which R_s decreases with higher moisture and temperature (Figs. 4–5). In our study area, soil temperature and moisture seldom reach these inflexion points in seasons other than summer, and subsequently the R_s of the biocrust and bare soil is much lower to negligible in the rest of the year (Fig. 6). Providing validation of our model, we also observed the R_s of biocrust across several days in winter (October 19–26 and December 1) with the same procedures, and the results showed that the R_s of biocrust averaged only 0.05 μmol m^{-2} s^{-1} (53.4% of the R_s were even negative) which was identical with the simulated results presented in Fig. 6B. Given the known threshold-dependency of R_s and our winter validation data, we believe that we obtained sufficient variation in soil temperature and moisture on which to base a model of R_s across the whole year and allow a comparison of values for biocrust and bare soil during the same time periods.

In this study, we obtained a R_s of 1.03 μmol m^{-2} s^{-1} averaged across all seasons (the highest value was 7.62 μmol m^{-2} s^{-1}) and estimated an annual CO_2-C emission of 390 g m^{-2} yr^{-1} for the moss-dominated biocrust in the Loess Plateau, which approximately equals the R_s of some representative vascular plant community types, including restored grassland (1.78–2.67 μmol m^{-2} s^{-1}; Wang et al., 2015; Zhang et al., 2015a), shrubland (0.84–3.71 μmol m^{-2} s^{-1}; Lellei-Kovács et al., 2016), forest land (2.35–3.23 μmol m^{-2} s^{-1}; Shi et al., 2014; Zhang et al., 2015a), and even cropland (1.26–1.90 μmol m^{-2} s^{-1}; Wang et al., 2015). Confirming the comparability of biocrust and vascular plant-driven R_s, Castillo-Monroy et al. (2011) indicated that the biocrust contribution to R_s (43%) in a semiarid *Stipa tenacissima* steppe was greater than that of vascular plants (37%) and bare soil (20%). Therefore, biocrust has a similar or sometimes even higher R_s than vascular plant communities in arid and semiarid climate regions. This finding strongly implies that the annual amount of C emission of biocrust cannot be ignored, and it should be taken into account in an accurate and comprehensive estimation of the C-balance in semiarid ecosystems.

4.2. Biocrust counterbalances greater C efflux with greater C storage

The higher R_s of the biocrust compared with bare soil does not mean the biocrust behaves as a net C source, because biocrust simultaneously sinks and stores much more C than bare soils (Table 3) depositing organic matter and creating “mantles of fertility” in the interspaces among vascular plants (Garcia-Pichel et al., 2003; Li et al., 2012). For example, Büdel et al. (2018) estimated that the cyanobacteria-dominated biocrust released 1.05 g CO_2-C m^{-2} yr^{-1} through dark respiration (this rate is much lower than the rate in our study, because the climate in that study area is usually cooler in comparison to the Loess Plateau), but they fixed 2.75 g CO_2-C m^{-2} yr^{-1} in total through photosynthesis and finally gained a net 1.70 g CO_2-C m^{-2} yr^{-1} in the north Queensland Gulf Savannah. The net photosynthetic rate of biocrust reaches as high as 11.5 μmol m^{-2} s^{-1} (CO_2) under optimal environmental conditions, which is comparable to the rates of some vascular plants (Lange, 2003).

In our study, the biocrust layer had 1.51–6.40 times higher content of different forms of C, suggesting that the contribution of the biocrust to R_s may have stemmed from decomposition of C previously fixed and stored in the biocrust. Pointing and Belnap (2012) suggested that biocrust creates a thin surface layer of high biotic activity, with high C and nutrient pools and fluxes relative to bare soil, where the soil tends to be biotically and biogeochemically less active. Although biocrust possibly increased R_s through various direct and indirect pathways, its much higher R_s may be attributable to a higher microbial biomass supported by accumulated C and N pools (Tables 3–4) fixed by biocrust

Table 2
Simulated soil respiration rate (R_s) of the biocrust and bare soil and their annual estimated CO_2-efflux.

Treatments	R_s (μmol m^{-2} s^{-1})						Repeated measures ANOVA			Annual CO_2 efflux (g m^{-2} yr^{-1})†
	Mean	S.E.	Max.	Min.	*CV*	*RMSE*	*MS*	*F*	*P*	
Biocrust	1.03	0.004	4.11	0.006	0.97	1.41	66.34	225.51	< 0.001	390
Bare soil	0.54	0.002	1.45	0.010	0.77	0.70				203

S.E. = Standard Error; *CV* = Coefficient of Variation; *RMSE* = Root Mean Square Error; *MS* = Mean Square.
† The period was from June 18, 2017 to June 17, 2018.

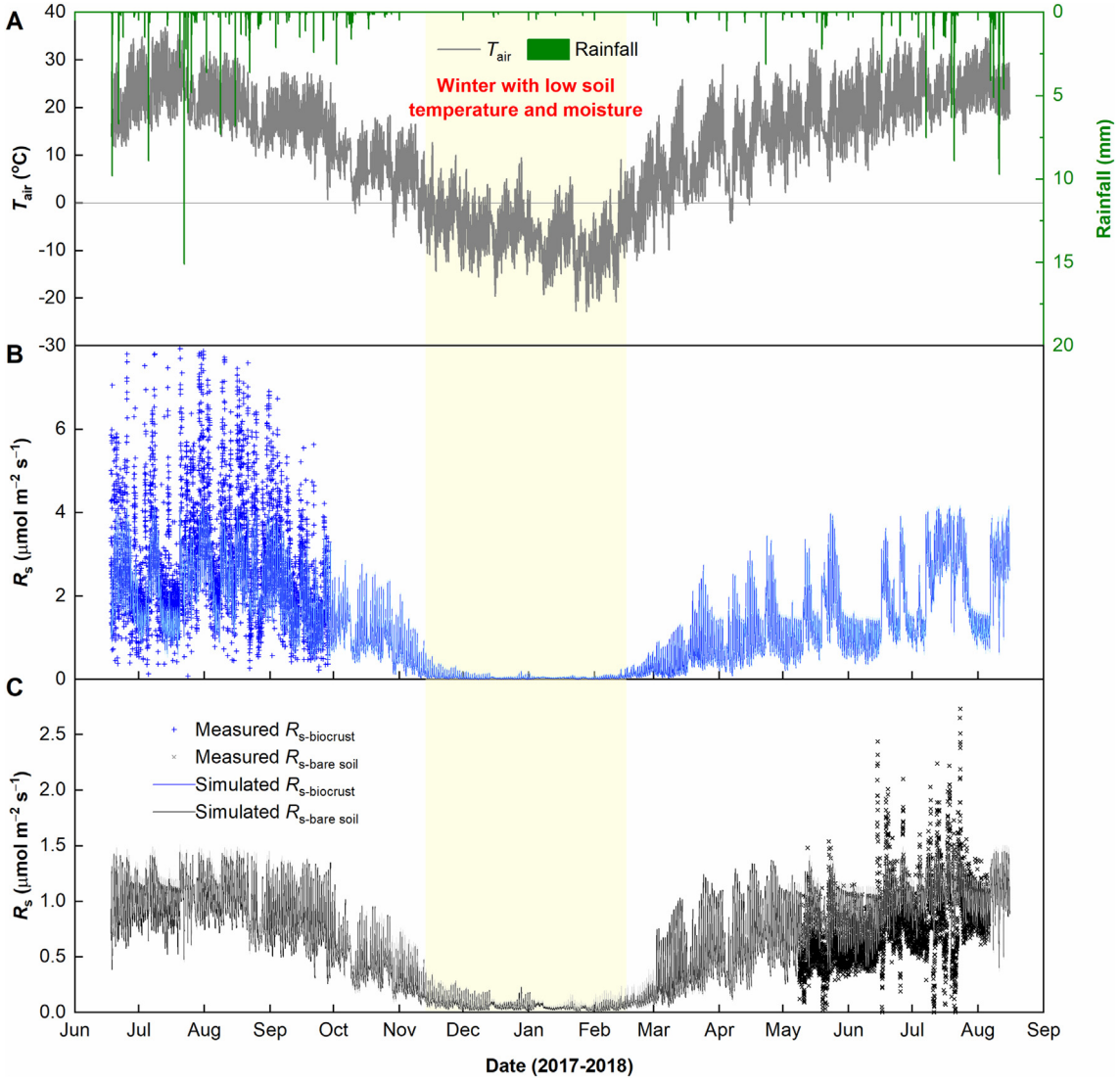

Fig. 6. Simulated soil respiration rate (R_s) of the biocrust and bare soil during the period from June 18, 2017 to August 15, 2018. (A) Air temperature (T_{air}) and rainfall; (B) Simulated R_s of the biocrust ($R_{s\text{-biocrust}}$); (C) Simulated R_s of the bare soil ($R_{s\text{-bare soil}}$). The shaded area represents the 95% confidence interval.

autotrophs. The fact that, despite higher R_s, a much higher C pool is retained in biocrust compared to bare soil (6.4 times higher as indicated by LOC and MBC; Table 3), indicates that biocrust is likely a net C sink, rather than a source.

4.3. Indirect mechanisms underlying biocrust enhancement of soil respiration

Biocrust contains much more autotrophic biomass than bare soils, thus it could directly influence R_s through enhanced autotrophic

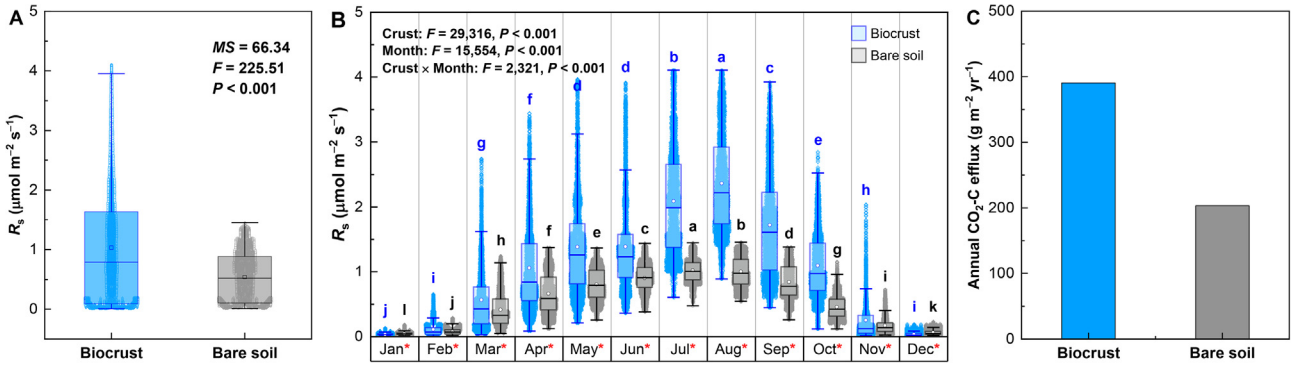

Fig. 7. Simulated soil respiration rate (R_s) and estimated annual CO_2-C efflux of the biocrust and bare soil. (A) Annual mean of R_s; (B) Seasonal variation of R_s; (C) Annual CO_2-C efflux. *Difference between the biocrust and bares soil is significant at 0.05 level of probability. Different letters presented in each soil treatment indicate significant differences among different months at 0.05 level of probability. *MS* = Mean Square.

Table 3
Physicochemical properties and enzyme activities of the biocrust and bare soil.

Measurements	Biocrust	Bare soil	*t*	*P*
Bulk density (g cm^{-3})	1.16 ± 0.06	1.57 ± 0.08	–24.60	**0.006**
Clay content (< 0.002 mm) (%)	0.78 ± 0.05	0.33 ± 0.09	12.53	**0.003**
Silt content (0.002–0.05 mm) (%)	21.68 ± 0.48	9.81 ± 0.72	38.94	**0.011**
Sand content (0.05–2.0 mm) (%)	77.54 ± 0.50	89.86 ± 0.80	–6.96	**0.004**
OC content (g kg^{-1})	2.84 ± 0.76	1.13 ± 0.49	4.60	**0.001**
LOC content (μg g^{-1})	315.23 ± 10.23	42.62 ± 2.67	63.11	< **0.001**
MBC content (μg g^{-1})	368.55 ± 5.37	49.88 ± 1.35	140.90	< **0.001**
TN content (g kg^{-1})	0.88 ± 0.05	0.17 ± 0.03	31.72	< **0.001**
AN content (mg g^{-1})	72.57 ± 2.64	23.99 ± 3.29	28.24	< **0.001**
MBN content (mg g^{-1})	1.43 ± 0.22	0.67 ± 0.05	8.41	< **0.001**
TP content (g kg^{-1})	0.39 ± 0.02	0.19 ± 0.02	15.72	< **0.001**
AP content (mg g^{-1})	5.59 ± 0.47	0.84 ± 0.20	23.05	< **0.001**
Urease (μg $g^{-1}h^{-1}$)	33.74 ± 5.82	9.60 ± 6.40	6.84	< **0.001**
Alkaline phosphatase (μg $g^{-1}h^{-1}$)	52.37 ± 10.67	10.22 ± 14.85	5.64	< **0.001**
Sucrase (μg $g^{-1}h^{-1}$)	591.43 ± 82.19	17.98 ± 5.00	17.06	< **0.001**
Catalase (μg $g^{-1}h^{-1}$)	5.97 ± 0.45	2.41 ± 1.42	4.13	**0.014**
Protease (μg $g^{-1}h^{-1}$)	14.27 ± 1.23	6.40 ± 0.62	14.02	< **0.001**
Peroxidase (μg $g^{-1}h^{-1}$)	699.88 ± 39.07	41.23 ± 5.37	22.57	< **0.001**
Polyphenol oxidase (μg $g^{-1}h^{-1}$)	318.15 ± 35.21	74.18 ± 30.93	8.65	< **0.001**

respiration. However, there are multiple additional ways in which biocrust influences the abiotic and biotic soil environment that could regulate heterotrophic respiration. Xu and Qi (2001) suggested that most (84%) of the spatial variation of R_s was expected due to the differences in soil properties, root density, and microbial activity in an 8-year-old ponderosa pine plantation; this explanation likely works for increased R_s in biocrust versus bare soil. In this study, we found that biocrust has a lower bulk density, finer texture, and higher organic matter content, microbial biomass, fertility and enzyme activity. In terms of soil physical properties, the R_s of biocrust may be enhanced by a greater prevalence of soil structural pores, which would improve soil aeration and subsequently change the population size and activity of the microbial community (Al-Kaisi and Yin, 2005). Moreover, the increasing content of silt particles (and concomitant decreasing content of sand particles) in biocrust likely improved nutrient retention, thus increasing microbial activity; the increased silt also possibly enhanced stability of soil macropores, which would accelerate microbial activity due to aeration and cause a more rapid loss of organic matter and enhancement of CO_2 flux (Xiao et al., 2019c; Yazdanpanah, 2016). In contrast, the high content of clay in soil provides potential for forming aggregates, and protection of SOC by the clay within aggregates, thereby potentially reducing CO_2 emissions (Chivenge et al., 2007); this general expectation may not be relevant in our study because the clay content of the soils was very low, and as a result it probably has a negligible effect on R_s. Additionally, the bulk density of biocrust decreases with increasing biocrust coverage, thickness or biomass, which would directly lead to the increase of R_s from mosses, or indirectly result in the increase of R_s by stimulating microbial activity (Maestre et al., 2005). Finally, biocrust could affect infiltration and evaporation, in turn impacting the moisture conditions (soil water content and wetness duration) of biocrust respiration (Kidron and Vonshak, 2012; Xiao et al., 2016).

In regard to soil chemical properties, biocrust had much richer content of different forms of C, N, and P in the biocrust layer as compared with the bare soil. Generally, soil microorganisms, which are responsible for the decomposition and mineralization of organic components, utilize some of the compounds contained in the residues as sources of nutrients and energy for their biomass formation (Geisseler et al., 2011). The presence of biocrust likely produced higher MBC due to the greater biomass, higher tissue turnover, and higher exudation rates (Liu et al., 2013). This effect might be interpreted as being akin to higher "rhizodeposition" quality around mosses. An increase in the contents of nutrients, such as TP and TN, would be expected to stimulate microbial activity and also microbial biomass cycling, thus resulting in an enhanced R_s (Emmerling et al., 2000). Higher microbial activity is readily observed when contrasting biocrust to bare soils, but surprisingly we found that the response of R_s to TP and TN was fundamentally different in bare and biocrust microsites. TN was strongly positively related to to R_s in biocrust samples, but not in bare samples, and TP was strongly negatively related to R_s in bare samples but not biocrust samples. This result is puzzling, but may relate to the very different nutrient stoichiometries in bare and biocrust samples with regards to TN and TP. For example, it is suggested biocrust and its extracted exopolysaccharides are able to sorb more nutrients and metabolites than bare soil (Swenson et al., 2018). Moreover, biocrust may buffer the effects of changes in nutrient ratios on microbial functional diversity, indicating that these organisms may have an important role in increasing the resilience of nutrient cycles to imbalances in C, N and P (Delgado-Baquerizo et al., 2013). Due to the microbial functional genes and enzyme activities, different types of biocrust and bare soil also have different mechanisms of soil nutrient transformation to changing environment such as warming and reduced precipitation (Hu et al., 2020). All of these would lead to significant differences in C, N, P concentrations and stoichiometric ratio between biocrust and bare soil, which possibly further lead to their different responses of R_s to soil nutrients in this study.

Table 4
Spearman correlation coefficients (significance in bracket) between the R_s and soil physicochemical properties of biocrust and bare soil.

Treatments	Clay (%)	Silt (%)	Sand (%)	Bulk density (g cm^{-3})	OC (g kg^{-1})	LOC (μg g^{-1})	MBC (μg g^{-1})	TN (g kg^{-1})	AN (mg g^{-1})	MBN (mg g^{-1})	TP (g kg^{-1})	AP (mg g^{-1})
Biocrust	0.09	−0.26	0.37	−0.52	−0.14	−0.71	0.54	0.93	−0.37	0.43	0.64	0.26
	(0.87)	(0.62)	(0.47)	(0.29)	(0.79)	(0.11)	(0.27)	(**0.008**)	(0.47)	(0.40)	(0.17)	(0.62)
Bare soil	−0.91	−0.93	0.93	0.04	0.41	0.06	−0.20	−0.63	−0.09	−0.23	−0.97	−0.06
	(**0.01**)	(**0.01**)	(**0.01**)	(0.93)	(0.42)	(0.91)	(0.70)	(0.18)	(0.87)	(0.66)	(**0.001**)	(0.91)

Note: *P* values equal or below 0.05 are in bold.

Table 5
Spearman correlation coefficients (significance in bracket) between the R_s and soil enzyme activities of biocrust and bare soil.

Treatments	Urease ($\mu g\ g^{-1}h^{-1}$)	Alkaline phosphatase ($\mu g\ g^{-1}h^{-1}$)	Sucrase ($\mu g\ g^{-1}h^{-1}$)	Catalase ($\mu g\ g^{-1}h^{-1}$)	Protease ($\mu g\ g^{-1}h^{-1}$)	Peroxidase ($\mu g\ g^{-1}h^{-1}$)	Polyphenol oxidase ($\mu g\ g^{-1}h^{-1}$)
Biocrust	−0.54 (0.27)	−0.89 (**0.02**)	−0.77 (0.07)	0.43 (0.40)	−0.67 (0.15)	−0.03 (0.96)	−0.26 (0.62)
Bare soil	−0.72 (0.10)	−0.67 (0.15)	−0.03 (0.96)	0.18 (0.73)	−0.06 (0.91)	−0.18 (0.73)	0.18 (0.73)

Note: *P* values equal or below 0.05 are in bold.

With regard to soil biological properties, our study showed R_s was closely related with the activity of different types of soil enzymes. Biocrust had much higher activities of all soil enzymes, thus its R_s is generally positively correlated with enzyme activities. However, a closer look within the biocrust and bare groups of samples suggested that some enzymes tend to correlate negatively with R_s. Soil enzymes are intimately involved in catalyzing reactions necessary for soil organic matter decomposition, nutrient cycling, energy transfer and so on; thus, soil enzymes generally make strong contributions to the total biological activities in the soil environment (Yao et al., 2006). Higher soil enzyme activity in biocrust likely indicates higher microbial activity (Liang et al., 2003) and microbial biomass cycling, potentially related to higher R_s (Borken et al., 2002; Ge et al., 2009). For example, Catalase can split hydrogen peroxide into molecular oxygen and water (Yao et al., 2006), and it provides oxygen and water for soil respiration. The enzymes that tend to negatively correlate with R_s within biocrust are more difficult to explain, but might hypothetically be indicative of fine scale spatial heterogeneity in nutrient limitation (Cheng et al., 2004). Phosphatase can hydrolyze some kinds of organic compounds of P into inorganic P (Ge et al., 2009), and we can hypothesize that there would be greater phosphatase activity where mineral phosphate values are lower. Similarly, urease is mostly involved in the hydrolysis of urea-type substrates (Yao et al., 2006), and might be more prevalent in microsites where mineral N is limiting. Thus, biocrust exhibits much more biological biomass and activity than bare soils, and the higher biomass also incurs greater nutrient demands. Within the biocrust microsites, relatively low nutrient availability might increase some enzyme activities but limit R_s, inducing a negative correlation between enzymes and R_s. This hypothesis will require further testing.

Finally, the presence of biocrust also impacts the soil moisture and temperature regimes (Xiao et al., 2016; Xiao et al., 2019a). Soil temperature is an important factor regulating the variations of soil enzymes and activities of microorganisms, which, in turn, controls soil CO_2 emissions; however, these influences mostly rely on an appropriate soil moisture (Cartwright and Hui, 2015; Ussiri and Lal, 2009). Generally, R_s increases with increasing soil moisture at the lower range of soil moisture but will decrease when soil moisture increases to a certain value (Deng et al., 2012; Hui and Luo, 2004). In our study, we found that the inflexion points of soil moisture of the biocrust and bare soil were different; they were 0.15 and 0.11 $cm^3\ cm^{-3}$, respectively, approximately accounting for 70% of the soil field capacity. Similar results were also reported by Castillo-Monroy et al. (2011) and Zhang et al. (2015b), who found that the threshold value was 0.25 and 0.11 $cm^3\ cm^{-3}$ for biocrust and bare soil, respectively. Moreover, it has been confirmed that the presence of biocrust significantly changed soil temperature and moisture regimes at depths of 0–30 cm (Xiao et al., 2016; Xiao et al., 2019a). Thus, the R_s of biocrust was interpreted to be indirectly influenced by biocrust effects on soil temperature and moisture, both in magnitude and soil-profile distribution. All these results suggest that the regulating effects of biocrust on soil environmental factors possibly make an indirect but also significant contribution to the increasing soil respiration.

5. Summary and conclusions

We estimated the annual CO_2 efflux of moss-dominated biocrust and bare soil through measuring and simulating their R_s in a semiarid climate on the Chinese Loess Plateau, which were 390 and 203 g CO_2-C $m^{-2}\ yr^{-1}$, respectively. In comparison to bare soil, biocrust contributed 91.8% more soil C efflux; therefore, biocrust contribution to soil respiration and C cycling should be sufficiently evaluated in drylands. Moreover, soil environmental factors including temperature and moisture explained most variations of R_s of both biocrust and bare soil; thus, they can be used to simulate the dynamic changes of R_s and to estimate the long-term CO_2 efflux of soil with or without biocrust, where continuous measurement of R_s is infeasible. Furthermore, we found that the presence of biocrust alters which soil properties and enzyme activities are most correlated to R_s, largely shifting from mostly abiotic factors to mostly biotic ones. Although more clarity is needed about the mechanisms by which biocrust increases R_s, we believe that biocrust effects on soil environmental conditions, soil nutrients, and microbial biomass are the most important pathways to investigate. Lastly, we should keep in mind that the higher R_s of biocrust does not mean that biocrust is a net C source, because it simultaneously stores much more C than bare soil, and it accrues over time, consistent with the behavior of a net C-sink.

Declaration of Competing Interest

The authors declare that they have no known competing financial interests or personal relationships that could have appeared to influence the work reported in this paper.

Acknowledgments

This study was funded by the National Natural Science Foundation of China (No. 41671221), the China Scholarship Council (No. 201906355019), and the “Light of West China” Program of the Chinese Academy of Sciences (No. 2019). The authors are grateful to the Shenmu Experimental Station of Soil Erosion and Environment, CAS & MOE for its logistical support. MAB was supported by the National Science Foundation’s Dimensions of Biodiversity Program (No. 1638966).

Appendix A. Supplementary data

Supplementary data to this article can be found online at https://doi.org/10.1016/j.geoderma.2020.114560.

References

Al-Kaisi, M.M., Yin, X.H., 2005. Tillage and crop residue effects on soil carbon and carbon dioxide emission in corn-soybean rotations. J. Environ. Qual. 34, 437–445.
Belnap, J., Büdel, B., 2016. Biological soil crusts as soil stabilizers. In: Weber, B., Büdel, B., Belnap, J. (Eds.), Biological Soil Crusts: An Organizing Principle in Drylands. Springer International Publishing, Cham, pp. 305–320.
Bond-Lamberty, B., Bronson, D., Bladyka, E., Gower, S.T., 2011. A comparison of trenched plot techniques for partitioning soil respiration. Soil Biol. Biochem. 43, 2108–2114.
Borken, W., Muhs, A., Beese, F., 2002. Application of compost in spruce forests: effects on soil respiration, basal respiration and microbial biomass. For. Ecol. Manage. 159, 49–58.
Büdel, B., Williams, W.J., Reichenberger, H., 2018. Annual net primary productivity of a cyanobacteria-dominated biological soil crust in the Gulf Savannah, Queensland, Australia. Biogeosciences 15, 491–505.

Carter, M.R., Gregorich, E.G., 2006. Soil Sampling and Methods of Analysis, Second ed. CRC Press, Boca Raton, USA.
Cartwright, J., Hui, D., 2015. Soil respiration patterns and controls in limestone cedar glades. Plant Soil 389 (1–2), 157–169.
Castillo-Monroy, A.P., Maestre, F.T., Soliveres, S., García-Palacios, P., 2011. Biological soil crust microsites are the main contributor to soil respiration in a semiarid ecosystem. Ecosystems 14 (5), 835–847.
Chae, N., Kang, H., Kim, Y., Hong, S.G., Lee, B.Y., Choi, T., 2016. CO_2 efflux from the biological soil crusts of the High Arctic in a later stage of primary succession after deglaciation, Ny-Ålesund, Svalbard, Norway. Appl. Soil Ecol. 98, 92–102.
Chamizo, S., Canton, Y., Lazaro, R., Sole-Benet, A., Domingo, F., 2012a. Crust composition and disturbance drive infiltration through biological soil crusts in semiarid ecosystems. Ecosystems 15, 148–161.
Chamizo, S., Cantón, Y., Miralles, I., Domingo, F., 2012b. Biological soil crust development affects physicochemical characteristics of soil surface in semiarid ecosystems. Soil Biol. Biochem. 49, 96–105.
Chamizo, S., Rodríguez-Caballero, E., Román, J.R., Cantón, Y., 2017. Effects of biocrust on soil erosion and organic carbon losses under natural rainfall. Catena 148, 117–125.
Cheng, X.L., An, S.Q., Liu, S.R., Li, G.Q., 2004. Micro-scale spatial heterogeneity and the loss of carbon, nitrogen and phosphorus in degraded grassland in Ordos Plateau, northwestern China. Plant Soil 259, 29–37.
Chivenge, P.P., Murwira, H.K., Giller, K.E., Mapfumo, P., Six, J., 2007. Long-term impact of reduced tillage and residue management on soil carbon stabilization: Implications for conservation agriculture on contrasting soils. Soil Tillage Res. 94, 328–337.
Delgado-Baquerizo, M., Morillas, L., Maestre, F.T., Gallardo, A., 2013. Biocrusts control the nitrogen dynamics and microbial functional diversity of semi-arid soils in response to nutrient additions. Plant Soil 372, 643–654.
Deng, Q., Hui, D.F., Zhang, D.Q., Zhou, G.Y., Liu, J.X., Liu, S.Z., Chu, G.W., Li, J., 2012. Effects of precipitation increase on soil respiration: A three-year field experiment in subtropical forests in China. PLoS ONE 7 (7), e41493.
Doran, J.W., Mielke, L.N., Power, J.F., 1990. Microbial activity as regulated by soil water-filled pore space, Transactions 14th International Congress of Soil Science, Kyoto, Japan, pp. 94-99.
Elbert, W., Weber, B., Burrows, S., Steinkamp, J., Büdel, B., Andreae, M.O., Pöschl, U., 2012. Contribution of cryptogamic covers to the global cycles of carbon and nitrogen. Nat. Geosci. 5 (7), 459–462.
Elbert, W., Weber, B., Büdel, B., Andreae, M.O., Pöschl, U., 2009. Microbiotic crusts on soil, rock and plants: Neglected major players in the global cycles of carbon and nitrogen? Biogeosciences 6 (4), 6983–7015.
Emmerling, C., Liebner, C., Haubold-rosar, M., Katzur, J., Schoder, D., 2000. Impact of application of organic waste materials on microbial and enzyme activities of mine soils in the Lusatian coal mining region. Plant Soil 22, 129–138.
Gao, L.Q., Bowker, M.A., Sun, H., Zhao, J., Zhao, Y.G., 2020. Linkages between biocrust development and water erosion and implications for erosion model implementation. Geoderma 357, 113973.
García-Palacios, P., Escolar, C., Dacal, M., Delgado-Baquerizo, M., Gozalo, B., Ochoa, V., Maestre, F.T., 2018. Pathways regulating decreased soil respiration with warming in a biocrust-dominated dryland. Glob. Change Biol. 24 (10), 4645–4656.
Garcia-pichel, F., Johnson, S.L., Youngkin, D., Belnap, J., 2003. Small-scale vertical distribution of bacterial biomass and diversity in biological soil crusts from arid lands in the Colorado Plateau. Microb. Ecol. 46 (3), 312–321.
Ge, G.F., Li, Z.J., Fan, F.L., Chu, G.X., Hou, Z.N., Liang, Y.C., 2010. Soil biological activity and their seasonal variations in response to long-term application of organic and inorganic fertilizers. Plant Soil 326, 31–44.
Ge, G.F., Li, Z.J., Zhang, J., Wang, L.G., Xu, M.G., Zhang, J.B., Wang, J.K., Xie, X.L., Liang, Y.C., 2009. Geographical and climatic differences in long-term effect of organic and inorganic amendments on soil enzymatic activities and respiration in field experimental stations of China. Ecol. Complex. 6 (4), 421–431.
Geisseler, D., William, R.H., Rainer, G.J., Bernard, L., 2011. Pathways of nitrogen utilization by soil microorganisms – a review. Soil Biol. Biochem. 42 (12), 2058–2067.
Gu, C., Jia, X.H., Wu, B., Cheng, L., Yang, Z.W., Yang, D.F., Zhao, X.B., 2017. Effect of simulated precipitation on the carbon flux in biological-soil crusted soil in alpine sandy habitats. Acta Ecol. Sin. 7 (13), 4423–4433 (in Chinese with English abstract).
Hu, R., Wang, X.P., Xu, J.S., Zhang, Y.F., Pan, Y.X., Su, X., 2020. The mechanism of soil nitrogen transformation under different biocrusts to warming and reduced precipitation: from microbial functional genes to enzyme activity. Sci. Total Environ. 722, 137849.
Hui, D.F., Luo, Y.Q., 2004. Evaluation of soil CO_2 production and transport in Duke Forest using a process-based modeling approach. Glob. Biogeochem. Cycles 18 (4), GB4029.
Hursh, A., Ballantyne, A., Cooper, L., Maneta, M., Kimball, J., Watts, J., 2017. The sensitivity of soil respiration to soil temperature, moisture, and carbon supply at the global scale. Glob. Change Biol. 23, 2090–2103.
Jiang, H., Deng, Q., Zhou, G., Hui, D., Zhang, D., Liu, S., Chu, G., Li, J., 2013. Responses of soil respiration and its temperature/moisture sensitivity to precipitation in three subtropical forests in southern China. Biogeosciences 10, 3963–3982.
Kidron, G.J., Li, X.R., Jia, R.L., Gao, Y.H., Zhang, P., 2015. Assessment of carbon gains from biocrusts inhabiting a dunefield in the Negev Desert. Geoderma 253–254, 102–110.
Kidron, G.J., Vonshak, A., 2012. The use of microbiotic crusts as biomarkers for ponding, subsurface flow and soil moisture content and duration. Geoderma 181–182, 56–64.
Lal, R., 2004. Carbon sequestration in dryland ecosystems. Environ. Manage. 33, 528–544.
Lange, O.L., 2003. Photosynthesis of soil-crust biota as dependent on environmental factors. In: Belnap, J., Lange, O.L. (Eds.), Biological Soil Crusts: Structure, Function, and Management. Springer, Berlin Heidelberg, Berlin, Heidelberg, pp. 217–240.
Lellei-Kovács, E., Botta-Dukát, Z., De Dato, G., Estiarte, M., Guidolotti, G., Kopittke, G.R., 2016. Temperature dependence of soil respiration modulated by thresholds in soil water availability across European shrubland ecosystems. Ecosystems 19 (8), 1460–1477.
Leon, E., Vargas, R., Bullock, S., Lopez, E., Panosso, A.R., La Scala, N., 2014. Hot spots, hot moments, and spatio-temporal controls on soil CO_2 efflux in a water-limited ecosystem. Soil Biol. Biochem. 77, 12–21.
Li, X.R., Zhang, P., Su, Y.G., Jia, R.L., 2012. Carbon fixation by biological soil crusts following revegetation of sand dunes in arid desert regions of China: a four-year field study. Catena 97, 119–126.
Li, X.D., Fu, H., Guo, D., Li, X.D., Wan, C.G., 2010. Partitioning soil respiration and assessing the carbon balance in a *Setaria italica* (L.) Beauv. cropland on the Loess Plateau, Northern China. Soil Biol. Biochem. 42 (2), 337–346.
Liang, Y.C., Yang, Y.F., Yang, C.G., Shen, Q.R., Zhou, J.M., Yang, L.Z., 2003. Soil enzymatic activity and growth of rice and barley as influenced by organic manure in an anthropogenic soil. Geoderma 115, 149–160.
Liu, E.K., Yan, C.R., Mei, X.R., He, W.Q., Bing, S.H., Ding, L.P., Liu, Q., Liu, S., Fan, T.L., 2010. Long-term effect of chemical fertilizer, straw, and manure on soil chemical and biological properties in northwest China. Geoderma 158 (3–4), 173–180.
Liu, Y.M., Li, X.R., Xing, Z.S., Zhao, X., Pan, Y.X., 2013. Responses of soil microbial biomass and community composition to biological soil crusts in the revegetated areas of the Tengger Desert. Appl. Soil Ecol. 65, 52–59.
Liu, Y.M., Yang, H.Y., Li, X.R., Xing, Z.S., 2014. Effects of biological soil crusts on soil enzyme activities in revegetated areas of the Tengger Desert, China. Appl. Soil Ecol. 80, 6–14.
Lloyd, J., Taylor, J.A., 1994. On the temperature dependence of soil respiration. Funct. Ecol. 8, 315–323.
Maestre, F.T., Escudero, A., Martinez, I., Guerrero, C., Rubio, A., 2005. Does spatial pattern matter to ecosystem functioning? Insights from biological soil crusts. Funct. Ecol. 19 (4), 566–573.
Makhuvha, M., Arellano, R.M., Harney, D.M.W., 2014. Determination of bulk density, methods and impacts, with a case study from Los Bronces Mine, Chile. Appl. Earth Sci. 123, 196–205.
Min, H., Ye, Y.F., Chen, Z.Y., Wu, W.X., Du, Y.F., 2001. Effects of butachlor on microbial populations and enzyme activities in paddy soil. J. Environ. Sci. Health, Part B 36, 581–595.
Morillas, L., Bellucco, V., Cascio, M.L., Marras, S., Spano, D., Mereu, S., 2017. Contribution of biological crust to soil CO_2 efflux in a Mediterranean shrubland ecosystem. Geoderma 289, 11–19.
Parkinson, J.A., Allen, S.E., 1975. A wet oxidation procedure suitable for the determination of nitrogen and mineral nutrients in biological material. Commun. Soil Sci. Plant Anal. 6, 1–11.
Pointing, S.B., Belnap, J., 2012. Microbial colonization and controls in dryland systems. Nat. Rev. Microbiol. 10 (8), 551–562.
Poulter, B., Frank, D., Ciais, P., Myneni, R.B., Andela, N., Bi, J., Broquet, G., Canadell, J.G., Chevallier, F., Liu, Y.Y., Running, S.W., Sitch, S., van der Werf, G.R., 2014. Contribution of semi-arid ecosystems to interannual variability of the global carbon cycle. Nature 509, 600–603.
Qi, Y., Xu, M., Wu, J.B., 2002. Temperature sensitivity of soil respiration and its effects on ecosystem carbon budget: nonlinearity begets surprises. Ecol. Model. 153 (1–2), 131–142.
Raich, J.W., Potter, C.S., Bhagawati, D., 2002. Interannual variability in global soil respiration, 1980–94. Glob. Change Biol. 8 (8), 800–812.
Rodríguez-Caballero, E., Belnap, J., Büdel, B., Crutzen, P.J., Andreae, M.O., Pöschl, U., Weber, B., 2018. Dryland photoautotrophic soil surface communities endangered by global change. Nature Geosci. 11, 185–189.
Rutherford, W.A., Painter, T.H., Ferrenberg, S., Belnap, J., Okin, G.S., Flagg, C., Reed, S.C., 2017. Albedo feedbacks to future climate via climate change impacts on dryland biocrusts. Sci. Rep. 7, 44188.
Saiya-Cork, K.R., Sinsabaugh, R.L., Zak, D.R., 2002. The effects of long term nitrogen deposition on extracellular enzyme activity in an Acer saccharum forest soil. Soil Biol. Biochem. 34, 1309–1315.
Schindlbacher, A., Wunderlich, S., Borken, W., Kitzler, B., Zechmeister-Boltenstern, S., Jandl, R., 2012. Soil respiration under climate change: prolonged summer drought offsets soil warming effects. Glob. Change Biol. 18, 2270–2279.
Shi, W.Y., Yan, M.J., Zhang, J.G., Guan, J.H., Du, S., 2014. Soil CO_2 emissions from five different types of land use on the semiarid Loess Plateau of China, with emphasis on the contribution of winter soil respiration. Atmos. Environ. 88, 74–82.
Soil Survey Staff, 1999. Soil taxonomy: A basic system of soil classification for making and interpreting soil surveys. 2nd edition. Natural Resources Conservation Service. U.S. Department of Agriculture Handbook 436.
Sparling, G.P., West, A.M., 1988. Modifications to the fumigation-extraction technique to permit simultaneous extraction and estimation of soil microbial C and N. Commun. Soil Sci. Plant Anal. 19, 327–344.
Swenson, T.L., Couradeau, E., Bowen, B.P., De Philippis, R., Rossi, F., Mugnai, G., Northen, T.R., 2018. A novel method to evaluate nutrient retention by biological soil crust exopolymeric matrix. Plant Soil 429, 53–64.
Tang, X.L., Liu, S.G., Zhou, G.Y., Zhang, D.Q., Zhou, C.Y., 2006. Soil-atmospheric exchange of CO_2, CH_4, and N_2O in three subtropical forest ecosystems in southern China. Glob. Change Biol. 12, 546–560.
Ussiri, D.A.N., Lal, R., 2009. Long-term tillage effects on soil carbon storage and carbon dioxide emissions in continuous corn cropping system from an alfisol in Ohio. Soil Tillage Res. 104, 39–47.
Wang, D., Liu, Y., Shang, Z.H., Tian, F.P., Wu, G.L., Chang, X.F., Warrington, D., 2015. Effects of grassland conversion from cropland on soil respiration on the semi-arid Loess Plateau, China. Clean-Soil, Air, Water 43 (7), 1052–1057.

Weil, R.R., Islam, K.R., Stine, M.A., Gruver, J.B., Samson-Liebig, S.E., 2003. Estimating active carbon for soil quality assessment: a simplified method for laboratory and field use. Am. J. Altern. Agric. 18 (1), 3–17.
Wu, W.X., Ye, Q.F., Min, H., 2004. Effect of straws from Bt-transgenic rice on selected biological activities in water-flooded soil. Eur. J. Soil Biol. 40, 15–22.
Xiao, B., Hu, K.L., Ren, T.S., Li, B.G., 2016. Moss-dominated biological soil crusts significantly influence soil moisture and temperature regimes in semiarid ecosystems. Geoderma 263, 35–46.
Xiao, B., Ma, S., Hu, K.L., 2019a. Moss biocrusts regulate surface soil thermal properties and generate buffering effects on soil temperature dynamics in dryland ecosystem. Geoderma 2019 (351), 9–24.
Xiao, B., Sun, F.H., Hu, K.L., Kidron, G.J., 2019b. Biocrusts reduce surface soil infiltrability and impede soil water infiltration under tension and ponding conditions in dryland ecosystem. J. Hydrol. 568, 792–802.
Xiao, D., Ye, Y.Y., Xiao, S.S., Zhang, W., He, X.Y., Wang, K.L., 2019c. Effects of tillage on CO_2 fluxes in a typical karst calcareous soil. Geoderma 337, 191–201.
Xu, M., Qi, Y., 2001. Soil-surface CO_2 efflux and its spatial and temporal variations in a young ponderosa pine plantation in northern California. Glob. Change Biol. 7 (6), 667–677.
Xu, M., Shang, H., 2016. Contribution of soil respiration to the global carbon equation. J. Plant Physiol. 203, 16–28.
Yao, X.H., Min, H., Lü, Z.H., Yuan, H.P., 2006. Influence of acetamiprid on soil enzymatic activities and respiration. Eur. J. Soil Biol. 42 (2), 120–126.
Yao, X.M., Xiao, B., Kidron, G.J., Hu, K.L., 2019. Respiration rate of moss-dominated biocrusts and their relationships with temperature and moisture in a semiarid ecosystem. Catena 183, 104195.
Yazdanpanah, N., 2016. CO_2 emission and structural characteristics of two calcareous soils amended with municipal solid waste and plant residue. Solid Earth 7, 105–114.
Yu, J., Glazer, N., Steinberger, Y., 2014. Carbon utilization, microbial biomass, and respiration in biological soil crusts in the Negev Desert. Biol. Fertil. Soils 50, 285–293.
Zhang, Y.J., Guo, S.L., Liu, Q.F., Jiang, J.S., Wang, R., Li, N.N., 2015a. Responses of soil respiration to land use conversions in degraded ecosystem of the semi-arid loess plateau. Ecol. Eng. 74, 196–205.
Zhang, Z.S., Dong, X.J., Xu, B.X., Chen, Y.L., Zhao, Y., Gao, Y.H., Hu, Y.G., Huang, L., 2015b. Soil respiration sensitivities to water and temperature in a revegetated desert. J. Geophys. Res. Biogeosci. 120 (4), 773–787.